

## **An Experimental Study of the Liquid Entrainment from Swelled Two-Phase Mixture Surface in a Reactor Vessel**

**Kyong-Won Seo, Hyeng-Kuk Kim, Chang-Hyun Kim, and Moon-Hyun Chun**

Korea Advanced Institute of Science and Technology

371-1 Kusong-dong, Yusong-gu, Taejon, 305-701, Korea

### **Abstract**

*An experimental study of liquid entrainment by rapid surface swelling of a two-phase mixture in a vessel has been performed. To investigate the effects of air flow rate and initial water level on the liquid entrainment, a series of experiments have been performed using air and water as working fluids. A total of 64 experimental liquid entrainment rate data have been obtained for various combinations of test parameters (i.e., six different initial water levels and varying air flow rates from 300 to 1,200 lpm) using two test vessels of the same height and different inner diameters ( $D = 0.15$  and  $0.30\text{m}$ , respectively) for vertical bubbly and churn-turbulent flow conditions.*

*An empirical correlation for the liquid entrainment rate,  $E$ , has been developed in terms of the superficial velocity of air, the initial water level, the density of gas, the surface tension, and the gravity. This correlation shows a good agreement with the present experimental data within 30% over a wide range of flow parameters.*

### **1. Introduction**

The entrainment is a consequence of dynamic interactions between the liquid and the flowing gas and this phenomenon may occur whenever two phases are brought into contact and when their relative motion is particularly large. The entrainment of liquid by gas phase may occur in technical equipments such as boilers, evaporators, rectification columns, nuclear reactors. The effects of entrainment are detrimental to the performance of these engineering systems. In evaporation, distillation, and absorption, it may cause serious loss of contamination of the products, or it may diminish the effective separation of liquid components. The presence of water droplets in the steam may cause water hammer in pipes and superheaters, or it may cause damage to a reciprocating engine or a turbine. In direct cycle water boiling reactors, droplets that leave the boiling interface carry highly radioactive volatile substances.

The Advanced Power Reactor 1400 (APR1400) has adopted an advanced design feature of a safety depressurization system (SDS) to rapidly depressurize the primary system in case of events beyond the

design basis accident such as Total Loss of Feed Water (TLOFW). An important aspect of the SDS design is the determination of the bleed capacity of the SDS connected to the pressurizer of a nuclear reactor and the level swelling of the reactor core. It is, therefore, a considerable interest to understand the factors that affect the entrainment and to be able to predict the amount of liquid carried away by the gas or vapor phase as a function of design characteristics and operational conditions of the system.

Sterman et al. (1958)	a) Vertical Flow b) Bubbly Flow	P= 1.7 ~18.5 Mpa H= 40cm~80cm	$E = 6.1 \times 10^9 \frac{Fr^{1.38}}{Ar^{1.1}} \left( \frac{\sqrt{s}}{\sqrt{g(r_f - r_g)}} / H_v \right)^{0.92}$
Schrock et al. (1986)	a) Vertical Flow b) Annular Two-Phase Flow	a) Air – Water D=3.76 mm, P <sub>0</sub> =112~543 kPa b) Air – Water D=6.32 mm, P <sub>0</sub> =104~170 kPa c) Steam – Water D=3.96 mm, P <sub>0</sub> =117~164 kPa	$Fr_g \left( \frac{r_g}{\Delta r} \right)^{0.5} = 0.395 \left( \frac{h_b}{d} \right)^{2.5}$
Ishii et al. (1989)	a) Horizontal Flow b) Annular Two-Phase Flow	Air-Water	$E_\infty = \tanh(7.25 \times 10^{-7} We^{1.25} Re_f^{0.25})$
Utsuno et al. (1998)	a) Horizontal Flow b) Annular-Mist Flow	P=3~9 Mpa Mass Flux = 500 ~ 2000 Kg/m <sup>2</sup> Heat Flux = 0.33 ~ 2.0 MW/ m <sup>2</sup> L <sub>boiling</sub> /D <sub>tube</sub> = 200~800.	$E_\infty = \tanh(0.16We^{0.08} Re_f^{0.16} - 1.20)$
Kataoka et al. (2000)	a) Horizontal Flow b) Annular Two-Phase Flow	Air – Water 20°C & 1 atm We = 2000, D = 0.01 m Re <sub>f</sub> = 100~10000	$\frac{ED}{m_f} = 6.6 \times 10^{-7} Re_f^{0.74} Re_{ff}^{0.185} We^{0.925} \left( \frac{m_g}{m_f} \right)^{0.26}$

Theoretical and experimental studies of the liquid entrainment have already been performed by a number of investigators in the past as summarized in Table 1. However, the liquid entrainments from

Table 1 Previous Works on Liquid Entrainment

Authors	Test Section Geometries & Conditions		Correlations for the Entrainment
	a) Flow Direction b) Flow Regime	Conditions	

a rapid swelling of two-phase mixture surface in a vessel has rarely been studied. Most of the existing correlations have a power-law relationship and the main test parameters are the flow rates of water and air, the surface tension, and the height of the vapor space.

According to Gordon et al. [1], Sterman examined the effect of the initial height of the vapor space upon the liquid entrainment in a vessel and proposed a correlation which takes this effect into account. By considering the equations of motion and energy, they obtained three dimensionless numbers of the Reynolds, the Froude, and the Weber. The entrainment rate has been approximated by a power law relationship. Schrock et al. [2] carried out an experimental study of liquid entrainment and pull-through in two-phase horizontal stratified flow in a small break loss of coolant accident (SBLOCA). For the case of an upward oriented break concerned with the present study, the correlation for the onset of entrainment was developed in terms of the gas Froude number and a non-dimensional interface height for both air-water and steam-water systems. Ishii et al. [3] carried out an analytical study of droplet entrainments in an annular two-phase flow. They considered that the amount of entrainment could significantly affect occurrences of dryout and post-dryout heat flux as well as the

rewetting phenomena of a hot dry surface. In view of these, a correlation for the amount of entrained liquid in an annular flow was developed from a simple model and experimental data obtained by other studies. The correlation for the equilibrium region was expressed in terms of the dimensionless gas flux, diameter of the test section, and the total liquid Reynolds number. Utsuno et al. [4] carried out an analytical study of droplet entrainment of liquid film to predict the critical heat flux (CHF) causing liquid film dryout in two-phase annular-mist flow in a uniformly heated narrow tube under BWR conditions. They modeled a two-phase annular-mist flow with the three-fluid streams of the liquid film, the entrained droplets and the gas flow. They proposed a correlation for the mass transfer which consists of the entrainment fraction at equilibrium and the mass transfer coefficient. Kataoka et al. [5] carried out an analytical study of droplet entrainment from a liquid film based on the previous work of Ishii et al. They proposed that the entrainment rate varied considerably in the entrainment development region but it attained an equilibrium value at a certain distance from an inlet. Also, they developed a simple approximate correlation for the equilibrium state where the entrainment rate and the deposition rate become equal and showed that the equilibrium entrainment rate was proportional to the Weber number based on the hydraulic diameter of the test section. Their correlation for the entrainment rate covers the entrance region as well as the equilibrium region.

## 2. Experiments

### 2.1 Experimental Apparatus

A schematic diagram of the experimental apparatus is shown in Fig.1. The present experimental apparatus has been designed to simulate an air-water vertical pipe flow. The main components of the system are the test vessel, an air supply system, a water reservoir and their associated piping systems, and the data acquisition system.

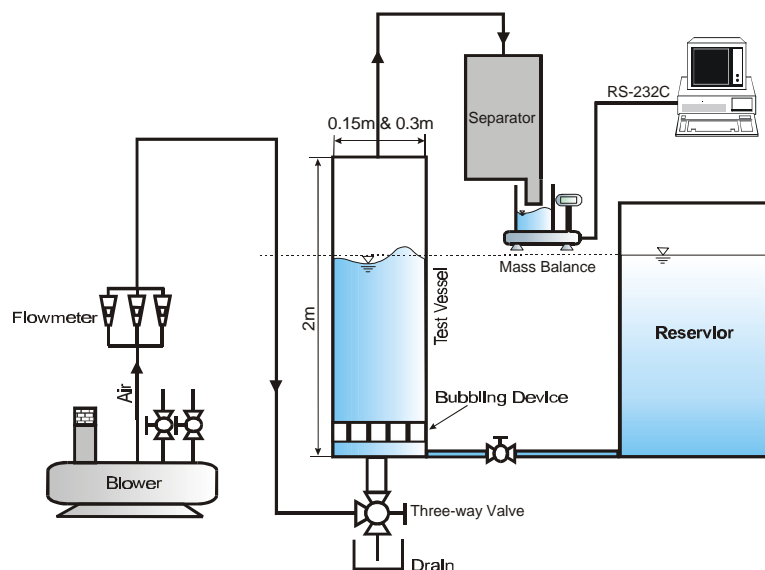


Fig. 1 Schematic Diagram of Experimental Apparatus

The test vessel is made of a 2 m long transparent pyrex pipe to enable visual observations of the flow pattern and variation of the liquid level. A series of experiments have been performed with two test vessels, one has an inner diameter of 0.15 m while the other has an inner diameter of 0.3 m. The test vessel was connected to a water reservoir to make up for the decrease of liquid level by liquid entrainments, and the top of the test vessel has a vent where the entrained water passes through, whereas an air supply system was connected to the lower part. In addition, a ruler was attached to the vessel wall for visual observations of the initial and varying water levels. At the bottom of the test vessel, a bubbling device, which has a number of small holes of 5 mm diameter, was installed to generate bubbles uniformly.

To prevent from an overflow of water from the test vessel, the top of the air supply pipe was placed at higher position than the test vessel. Also, an air-water separator was connected to the vent of the test vessel to protect the measurement device against the splash and a direct contact with the two-phase mixture flowing at a high velocity.

The data acquisition system consists of a PC and an A&D HP-60K electric balance with resolution of 1 gram. The weight of the entrained water was measured by an online electric balance and recorded by the PC connected to the balance.

## 2.2 Test Parameters and Test Matrix

The amount of entrained water was measured using the mass balance, whereas the two-phase mixture level and the level swelling are determined by visual observations. The air flow rate was controlled by a ball valve and measured by rotameters. The pressure of the air was maintained at constant value of about 5 bars.

A series of experiments have been carried out varying the air flow rate and the initial water level at atmospheric conditions. The experimental ranges of the air flow rate and the relative initial water level are  $5.945 \times 10^{-3} \sim 2.378 \times 10^{-2}$  kg/s (300~1,200 lpm) and 20~70%, respectively. Diameters of test vessels are 0.15 m (test section A) and 0.30 m (test section B), respectively. The test matrix of the present experiments is listed in the Table 2.

Table 2 Test Matrix

Test Section	$D_{vessel}$ (m)	$H_L/H_T$ (%)	$Q_{air}$ (lpm)	$j_g$ (m/s)
A	0.15	20, 30, 40, 50, 60, 70	300 ~ 1,200	0.283~1.132
B	0.30	20, 30, 40, 50, 60, 70	300 ~ 1,200	0.095~0.283

### 3. Results and Discussion

A total of 64 liquid entrainment rate data from the two-phase mixture surface in a vessel have been obtained at the atmospheric pressure, varying the test parameters of the inlet air flow rate, the initial water level, and the test section diameter.

#### 3.1 *Two-Phase Mixture Level Swelling and Entrainment*

In the present experiments, the level swelling of the two-phase mixture was determined by visual observations. The liquid level swelling and the liquid entrainment occurred due to a large specific volume of rising air bubbles at extremely higher velocities compared to that of liquid. In the present experiment, two flow patterns were observed as follows:

(1) For low air flow rate regions ( $<600$  *lpm*), the flow pattern is similar to the pure bubbly flow. The behavior of individual bubbles is quite the same as that of single bubbles rising in a vessel. An instantaneous picture shows that the flow pattern is nearly homogeneous, except for the small spatial non-uniformity such as liquid circulations. The bubble size distribution is unimodal (all bubbles have nearly the same size) and the liquid turbulence is confined to the wakes of individual bubbles. The surface of two-phase mixture slightly moves up and down and many droplets are generated by bursting bubbles. In the lower air flow rate region, therefore, most of the entrainment occurred in the form of droplets.

(2) For high air flow rate regions ( $\geq 600$  *lpm*), the churn-turbulent flow is observed. This flow is not truly dispersed but shows a chaotic and very intermittent behavior. It is observed that fast rising large bubbles co-exist with small bubbles. The bubble size distribution is therefore bimodal, and an instantaneous picture shows that this flow pattern is very heterogeneous. The two-phase mixture surface swells disorderly.

#### 3.2 *Liquid Entrainment into Vent*

Increase in the air flow rate in the vessel causes the interface of liquid to be unstable. The level of two-phase mixture swells due to the rising air flow. The droplets and liquid sheets are generated by bubble bursting and splashing on the swelling surface. Some of the droplets generated and liquid sheets reach to the top of the vessel and they were entrained into the vent depending on the air discharge rate through the vent and the interface level.

#### 3.3 *Onset of Entrainment*

In the present study, the point where the onset of liquid entrainment occurs has been chosen as the liquid level where liquid entrainment begins. The data for the test section A have been correlated

reasonably well in terms of the gas Froude number and a non-dimensional liquid height for the air-water system as shown in Fig.2. The correlation for test section A is obtained as follows:

$$Fr_g = 1.458e^{-0.2316(H_L/d)} \quad (1)$$

The experimental data for the test section B was difficult to correlate because the number of data taken for the onset of entrainment was not sufficient. It is, therefore, necessary to perform more experiments for higher air flow rates with larger capacity blower than those used in the present experiment.

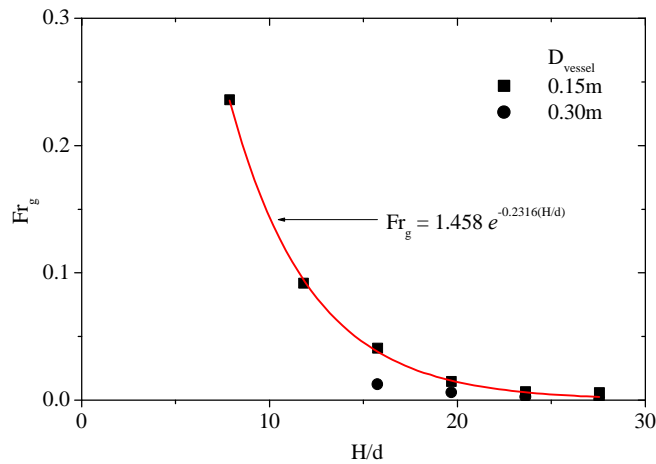


Fig. 2. Onset of Liquid Entrainment

### 3.4 Parametric Effects of Air Flow Rate and Initial Water Level

In Fig.3, the fraction of entrained water versus time is shown for two different air flow rates and three different initial water heights. In Fig.4, on the other hand, the entrainment rate (or mass flow rate of liquid over mass flow rate of air) versus superficial velocity of the inlet air is shown for different  $H_L/D$ . From these figures, the effects of inlet air flow rates on the liquid entrainment can be deduced. For the test section A, the entrained water fraction increases with the air superficial velocity as can be seen in Fig.3. Entrained water fraction rises rapidly up to 30% of the relative water height because the two-phase mixture level swells as the air blows into the vessel and the probability of entrainment of liquid sheets and droplets by air becomes larger due mainly to the very small distance between the collapse level and the vent. Thereafter, the entrained water fraction increases almost linearly above 30%. For the test section B, the entrained water fraction increases as the superficial velocity of air increases as shown in Fig.3.

The entrainment rate as functions of superficial velocity of the inlet air and a non-dimensional initial water level is shown in Fig. 4. For a given initial liquid level, the liquid entrainment rate increases as the superficial air velocity increases in the low superficial air velocity region but it becomes constant at higher superficial air velocity region. The main reason for this may be due to

the fact that as the air flow rate becomes larger, the probability of entrainment of liquid sheets and droplet by the air becomes constant regardless of the initial water level.

The effect of the initial water level on the liquid entrainment is shown in Fig.5. For a given superficial velocity of air, the liquid entrainment rate increases as the initial water level increases. However, the effect of superficial velocity is relatively small in the region of high water level. The reason for this is because as the initial water level becomes higher, the probability of entrainment of liquid sheets and droplets by the high velocity air becomes constant regardless of the flow rate of air.

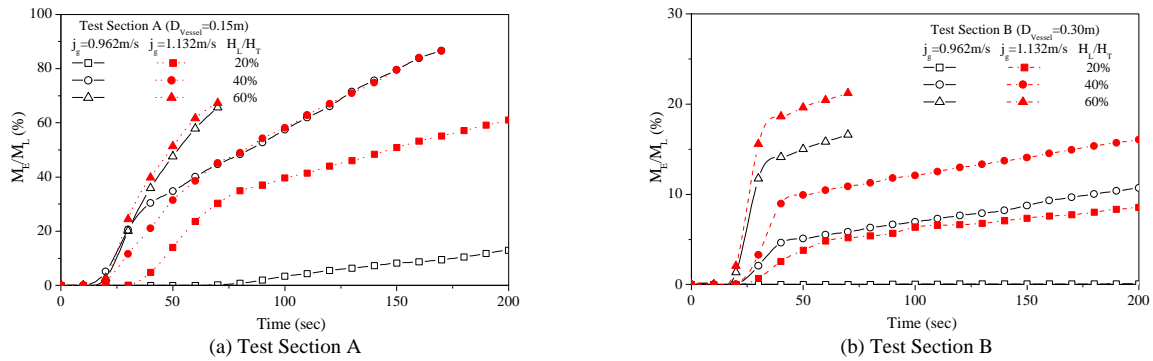


Fig. 3. Effects of Air Flow Rate on Entrainment: (Entrainment Fraction versus Time for Different Air Flow Rates and Different Initial Water Heights)

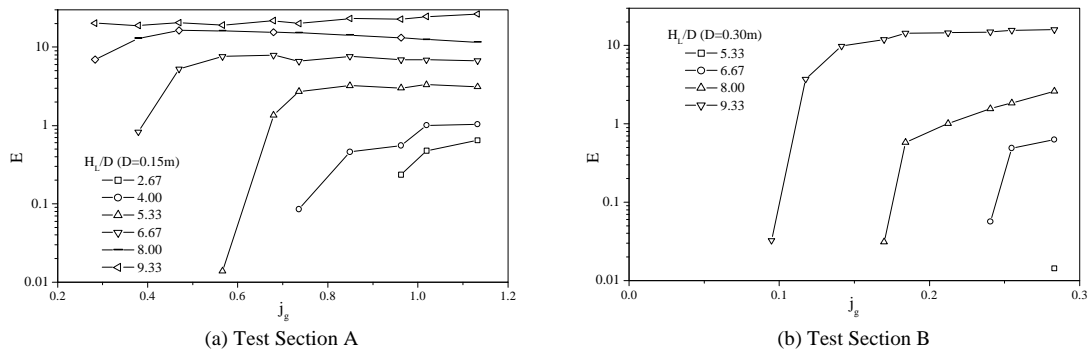


Fig. 4. Effect of Air Flow Rate on Entrainment Rate (Entrainment Rate versus Superficial Inlet Air Velocity for Various Initial Water Level)

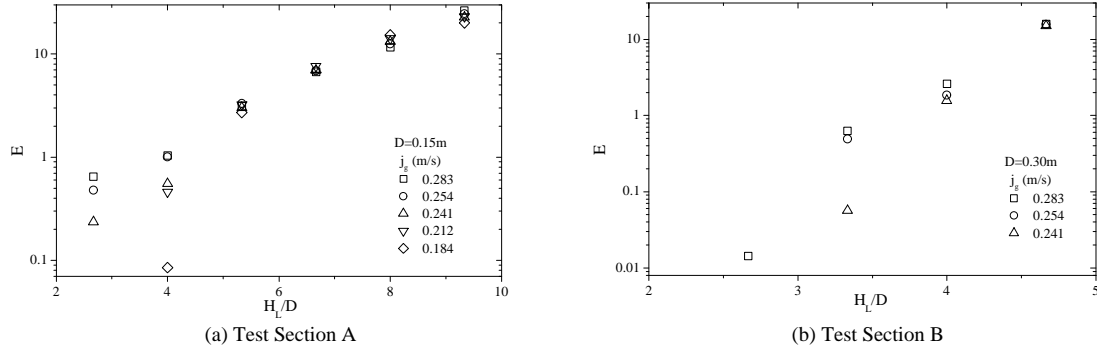


Fig. 5. Effect of Initial Water Level on Entrainment Rate: (Entrainment Rate versus Initial Water Level for Various Inlet Air Flow Rates)

### 3.5 Development of Empirical Correlation

Based on the present experimental data, an empirical correlation for the liquid entrainment rate from swelled two-phase mixture surface in a vessel has been developed by the dimensional analysis.

It is assumed that the liquid entrainment mainly depends on  $H_L$ ,  $\mathbf{r}_g$ ,  $j_g^2$ ,  $\mathbf{s}$ ,  $g$ , and  $D$ .

From the dimensional analysis, the following dimensionless groups were obtained:

$$\mathbf{p}_1 = \frac{g H_L}{j_g^2} \quad (2)$$

$$\mathbf{p}_2 = \frac{j_g^2 \mathbf{r}_g H_L}{\mathbf{s}} \quad (3)$$

$$\mathbf{p}_3 = \frac{H_L}{D} \quad (4)$$

The liquid entrainment rate is, therefore, expressed as a functions of  $\mathbf{p}_1$ ,  $\mathbf{p}_2$  and  $\mathbf{p}_3$  as follows:

$$E = C_1 f \left( \frac{g H_L}{j_g^2}, \frac{j_g^2 \mathbf{r}_g H_L}{\mathbf{s}}, \frac{H_L}{D} \right) \quad (5)$$

Finally, an empirical correlation has been obtained as follows:

$$E = 1.07 \times 10^{-3} \left( \frac{g H_L}{j_g^2} \right)^{1.348} \left( \frac{j_g^2 \mathbf{r}_g H_L}{\mathbf{s}} \right)^{-1.496} \left( \frac{H_L}{D} \right)^{0.723} \quad (6)$$

A comparison between the entrainment rate predicted by Eq.(6) and the measured entrainment rate is shown in Fig. 6. The present empirical correlation agrees with 78% of the measured data within 30% over a wide range of flow parameters.



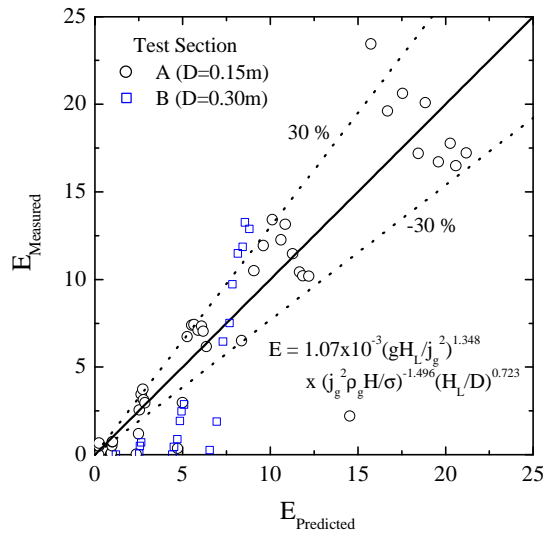


Fig. 6. Comparison of Predicted Entrainment Rate with Measured Data

#### 4. CONCLUSIONS

The liquid entrainment from a swelled two-phase mixture surface in a reactor vessel has been experimentally investigated and an empirical correlation has been developed. In the present experiment, the two patterns of level swelling of two-phase mixture have been observed. For lower air flow rates ( $<600 \text{ lpm}$ ), the flow pattern is similar to the pure bubbly flow. Most of the entrainment occurred by droplets that were generated by bursting bubbles. For higher air flow rates ( $\geq 600 \text{ lpm}$ ), on the other hand, the churn-turbulent flow is observed and the two-phase mixture surface swelled disorderly. It is observed that some of droplets and liquid sheets reach to the top of vessel and they are transferred and entrained into the vent depending on the air discharge rate through the vent and the interface level.

The onset of entrainment data have been obtained and they are correlated reasonably well in terms of the gas Froude number and the non-dimensional liquid height. The effects of the air flow rate and the initial water level on the liquid entrainment have also been examined. The entrained water fraction increases as the superficial air velocity increases. For a given non-dimensional initial liquid level, the liquid entrainment rate increases as the superficial air velocity increases in the low superficial air velocity region but it becomes constant at higher superficial air velocity region. Also, it has been observed that for a given superficial velocity of air, the liquid entrainment rate increases as the initial water level increases. The liquid entrainment becomes almost constant for high water level regions regardless of superficial air velocity.

From a total of 64 liquid entrainment rate data, an empirical correlation has been developed and 78% of present data agree with the present correlation within 30%.

## References

1. Gordon C. K. and Novak Zuber, "On The Problem of Liquid Entrainment," Argonne National Laboratory Subcontract 31-109-38-1159, 1960.
2. V. E. Schrock, S. T. Revankar, R. Mannheimer, and C. H. Wang, "Small Break Critical Discharge - The Roles of Vapor and Liquid Entrainment in a Stratified Two-Phase Region Upstream of the Break," NUREG/CR-4761, 1986.
3. M. Ishii and K. Mishima, "Droplet Entrainment Correlation in Annular Two-Phase Flow," *Int. J. Heat Mass Transfer*, Vol.**32**, No.10, pp.1835~1846, 1989.
4. H. Utsuno and F. Kaminaga, "Prediction of Liquid Film Dryout in Two-Phase Annular-Mist Flow in a Uniformly Heated Narrow Tube Development of Analytical Method under BWR Condition," *J. Nuclear Science and Technology*, Vol.**35**, No.9, pp.643-653, 1998.
5. I. Kataoka, M. Ishii, and A. Nakayama, "Entrainment and Deposition Rates of Droplets in Annular Two-Phase Flow," *Int. J. Heat Mass Transfer*, Vol.**43**, pp.1573-1589, 2000.